Experimental parameters for plasma wakefield acceleration in a narrow plasma column

Journal of Physics: Conference Series **3124** (2025) 012009 doi:10.1088/1742-6596/3124/1/012009

Experimental parameters for plasma wakefield acceleration in a narrow plasma column

V Lee[1*], S Diederichs[24], R Ariniello[3], C Benedetti[4], E Esarey[4], S Gessner[3], M Hogan[3], B O'Shea[3], J Osterhoff[24], C S chroeder[4], D Storey[3], M Thévenet[2], M Litos[1]

[1]Department of Physics, University of Colorado Boulder, Boulder, CO 80309, USA
[2]Deutsches Elektronen-Synchrotron DESY, Notkestr. 85, 22607 Hamburg, Germany
[3]SLAC National Accelerator Laboratory, 2575 Sand Hill Rd, Menlo Park, CA 94025, USA
[4]Lawrence Berkeley National Laboratory, 1 Cyclotron Rd, Berkeley, CA 94720, USA

Abstract. Recent theoretical advancements propose multiple positron acceleration schemes in plasma wakefield acceleration (PWFA). One of the most promising ideas involves the creation of an electron-driven blowout wake within a finite-radius pre-ionized plasma column. This leads to the formation of an elongated region of sheath electrons at the closing of the first wake period capable of accelerating positrons while simultaneously providing a transverse focusing force. Additionally, the proposed scheme has shown to be a potential means of suppressing instabilities. We present an experimental opportunity to explore the narrow column PWFA at the Facility for Advanced Accelerator Experimental Tests II (FACET-II): the E333 experiment. As a pivotal first step towards achieving positron acceleration in PWFA, we have planned a precursor experiment utilizing the currently available single-bunch electron beam to study the physics of the narrow plasma PWFA scheme. We outline the feasible experimental parameters, including beam and ionization laser parameters, along with the required laser optics for the experiment. The primary observable signatures for this stage of the experiment are the final energy spectrum and transverse position of the electron bunch, anticipating reduced energy loss and enhanced beam guidance in the narrow plasma column compared to the nominal PWFA. Comprehensive simulations are used to detail our experimental plan.

1. Introduction

Electron beam-driven plasma wakefield accelerators (PWFA) have demonstrated accelerating gradients orders of magnitude greater than that of conventional particle accelerators [1]. Much of the current research in the field is focused on realizing a PWFA with high energy efficiency and high beam quality [2, 3, 4]. In recent years, there has been growing interest in positron acceleration in a PWFA for the purpose of building a future plasma-based electron-positron collider [5].

1.1. Positron PWFA

The PWFA scheme for electron acceleration cannot be directly translated to positron acceleration. In the nominal electron-driven PWFA, a dense electron bunch drives a strong wake in a pre-ionized, uniform plasma, the transverse size of which is much larger than the blowout radius. The electric field from the drive electron beam expels plasma electrons from near the central axis of propagation forming a bubble-shaped region void of electrons behind it

* Valentina.Lee@colorado.edu

surrounded by a thin, dense plasma electron sheath [6]. This formation constitutes the plasma wake. Within the bubble, the electrostatic Coulomb field of the ions provides a radial force that is focusing for electrons but defocusing for positrons. Therefore, the conventional method of loading a trailing electron bunch inside the bubble region of the blowout wake is not practical for the acceleration of positrons.

Several schemes for positron acceleration in a PWFA have been demonstrated experimentally. These include positron acceleration in the linear wakefield regime [7], positron-driven acceleration of positrons in the nonlinear suck-in regime [8], and positron acceleration in a hollow column PWFA [9, 10, 11]. Each scheme presents its own advantages and obstacles, but one of the common challenges arises from the lack of well-controlled focusing during the acceleration of the positrons.

Remarkably, there exists a wake phase within the nominal blowout PWFA scheme that is simultaneously accelerating and focusing for positrons. This phase occurs when the sheath electrons cross through the central axis at the rear of the first (and each subsequent) wake period [12, 13], as shown in Fig. 1 (a-c). This phase, however, is very short, making it a difficult target for the loading of positron bunches. In the subsequent subsection, we introduce a scheme designed to extend this wake phase, thereby enhancing its feasibility for positron acceleration.

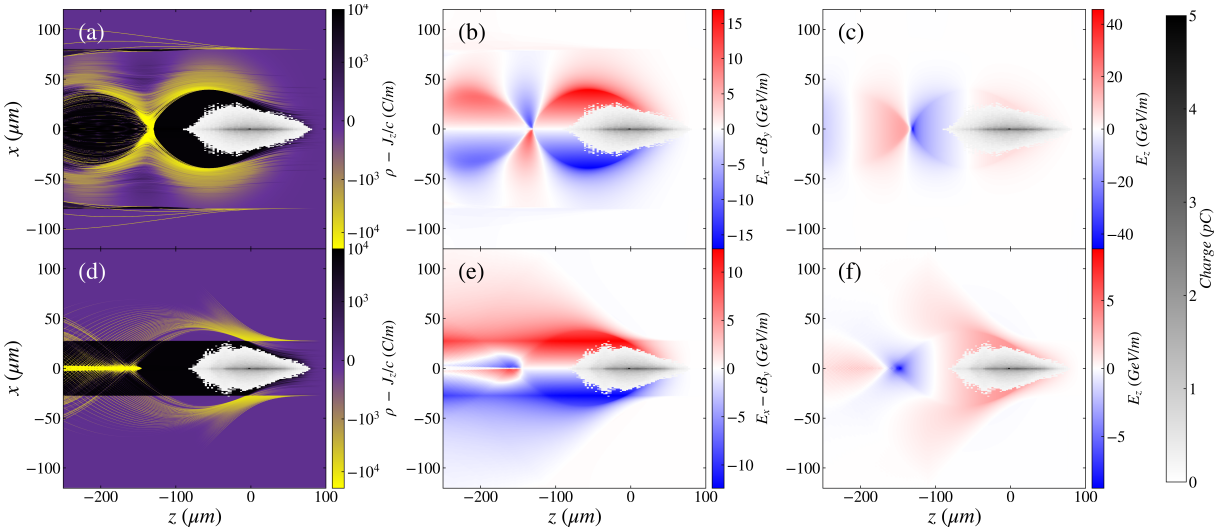

Figure 1. 3D Particle-in-cell (PIC) simulations of a wide- and narrow-column PWFA, conducted with a quasi-static, 3D PIC code, HiPACE++ [14]. The complete numerical settings for the simulations in this paper are available online [15]. (a), (b), and (c) show the plasma electron density, transverse focusing field, and longitudinal electric field, respectively, from a nominal (wide plasma column) PWFA. The black/white colormap in each subfigure shows the density of the drive electron beam. The density of the pre-ionized plasma is $5 \times 10^{16} cm^{-3}$ and the radius of the plasma column is $80\,\mu$m. (d), (e) and (f) show the simulation output for a narrow plasma column ($r_p = 27.5\,\mu$m) PWFA. (d) shows that the narrow-column PWFA creates an elongated electron filament in the rear of the wake, whereas the sheath electrons collapse to a point-like structure in the nominal wide-column PWFA.

1.2. Positron Acceleration in a Narrow Plasma column

Recently, a new positron acceleration scheme has been proposed and demonstrated in simulations by Diederichs and Benedetti, et al [16]. The authors propose driving a nonlinear blowout wake in a finite-radius plasma column using a relativistic electron beam, with the column width

Table 1. Current FACET-II single bunch beam parameters.

Variables	Values
Energy	10 GeV
Charge	1.5 nC
Emittance $\epsilon_{x,y}$	10, 10 μm rad
RMS Bunch Length σ_ζ	20 μm
RMS Beam Size σ_r	20 μm
Energy Spread σ_δ	1 %

slightly smaller than the blowout radius. The limited size of the ion column causes the sheath electrons to return to different longitudinal positions based on their initial transverse positions. This scheme creates an elongated electron filament in the rear of the wake that provides a transverse focusing field within the wake phase that is accelerating for positions as shown in Fig. 1(d-f). This concept is well supported by simulation results, and has been explored in the context of positron acceleration and transportation [17, 18]. The narrow plasma scheme has also been shown to suppress the hosing instability in the electron drive bunch [19]. In this work, we present a set of feasible experimental parameters to realize the first electron-driven narrow plasma column PWFA tests at The Facility for Advanced Accelerator Experimental Tests II (FACET-II).

2. Experimental Facility and Plan

2.1. FACET-II Facility

FACET-II is a user facility at SLAC National Accelerator Laboratory dedicated to advanced particle accelerator research, designed to provide electron beams with a single or double bunch configuration at 10 GeV, with up to ∼2 nC of total charge, ∼10 kA peak current, and 5 μrad emittance at a repetition rate of 10 Hz [20]. Currently, FACET-II is in the final commissioning phase, and a moderate-quality single-bunch electron beam is available. Table 1 shows the expected beam parameters for the upcoming run time in Spring 2024.

The E333 experiment and other PWFA experiments (e.g., E301) at FACET-II share a similar experimental setup, as shown in Fig. 2. A high-power laser is focused by a focusing lens to an unconfined gas, ionizing a meter-long plasma in the Bypass Line in Fig. 2. An electron beam is delivered several picoseconds behind the laser pulse. The interacting point of the laser-ionized plasma and e-beam starts at roughly 1.5 m downstream of the final focusing optic (Tandem lens B in Fig. 2). The spatial constraint from the pre-existed beam line hardware and the desired plasma source (plasma density and geometry) determine the design of the laser focusing optics. The electron spectrometer diagnostics are located downstream of the plasma-e-beam interaction, including an imaging spectrometer with various screens of different resolutions, sensitivities to different part of spectra, and fields of view for detecting the dispersed electron beam. The details of the experimental area and the available diagnostics at FACET-II can be found in Ref. [21].

2.2. The E333 Experiment

The primary scientific goal of the E333 experiment at FACET-II is to demonstrate controlled positron acceleration in a plasma wakefield accelerator [23]. There are 4 phases to this experiment: Phase 0 aims to develop and characterize the narrow plasma source. In Phases 1 and 2, we will study the electron-driven wakefield in a narrow plasma column using a single electron bunch, and a double electron bunch (drive and witness), respectively. Finally, in Phase 3, we aim to accelerate positrons in an electron-driven, narrow-column PWFA. Currently, FACET-

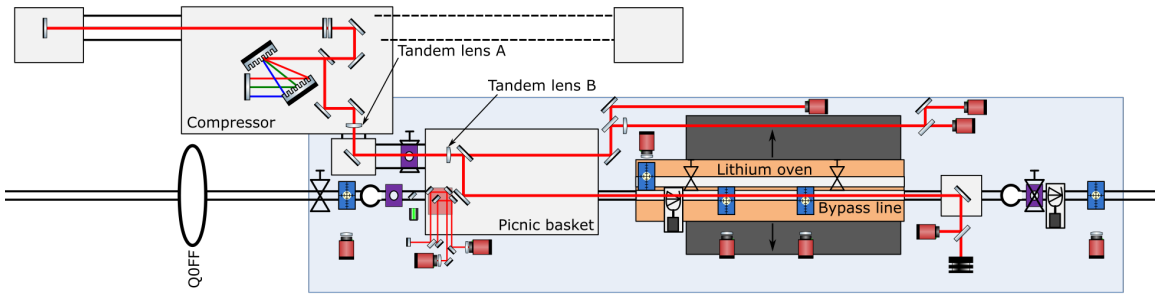

Figure 2. Experimental setup at FACET-II [22]. The red lines indicate the path of the high-intensity laser, entering the interaction point (IP) area (light blue) from the top left corner. The laser beam is focused by a custom-designed tandem lens pair (Tandem Lens A and Tandem Lens B), generating a plasma source within the "Bypass Line", a vacuum pipe parallel to the Lithium oven that can be moved into the beam path. The details of the optical setup is discussed in subsection 3.2. Electron beams traverse from left to right, focused by the final focusing system, of which only the final magnet (Q0FF) is shown. While not depicted in this figure, the electron diagnostic systems are detailed in Ref. [21].

II does not have the capability to provide positron beams, but plans have been devised for a future upgrade that would enable the injection of 10 GeV positrons simultaneously with the 10 GeV electrons in a drive-witness configuration. Despite the current absence of a positron beam, Phases 0, 1, and 2 of the E333 experiment can still be conducted at FACET-II using only the electron beam.

Here, we present an experimental plan for Phases 0 and 1 that can be carried out over the next year using a single electron bunch. In Section 3, we select the experimental parameters (e.g., the laser and gas parameters), considering beam ionization, optics, and the general requirements of the plasma source. Section 4 presents a study of experimental jitter tolerance using PIC simulations. Finally, we present our conclusions in Section 5 and discuss future work necessary to fully realize the E333 experiment.

3. Single Bunch Experimental Plan and Parameters

3.1. Beam Ionization

Strict control of the ionization laser intensity profile is crucial to realizing the narrow column PWFA plasma source. To maintain the designed geometry of the plasma source, beam ionization beyond the pre-ionized radius must be prevented. We use the ADK model [24] to calculate the degree of field ionization for various transverse and longituidnal dimensions of the electron beam in Hydrogen and Helium gas. The results, depicted in Fig. 3, indicate that a Gaussian beam with the current FACET-II beam parameters, $\sigma_{x,y,z} = 20$ μm, is incapable of ionizing Hydrogen or Helium. Consequently, it does not widen the pre-ionized narrow plasma column. However, it's important to note that structure on top of the nominal Gaussian shape assumed here can in fact lead to ionization of Hydrogen and Helium, even when the resolution limited measurements suggest that ionization will not occur. This structure can be due to beam jitter and/or microbunching. Therefore, careful beam tuning is required to succeed in this experiment [25].

3.2. Plasma Source

The plasma source in this experiment is ionized by a 50 fs, 300 mJ pulse from a terawatt-class Ti:Sapphire laser system. A custom-designed tandem lens pair is used to create both the nominal

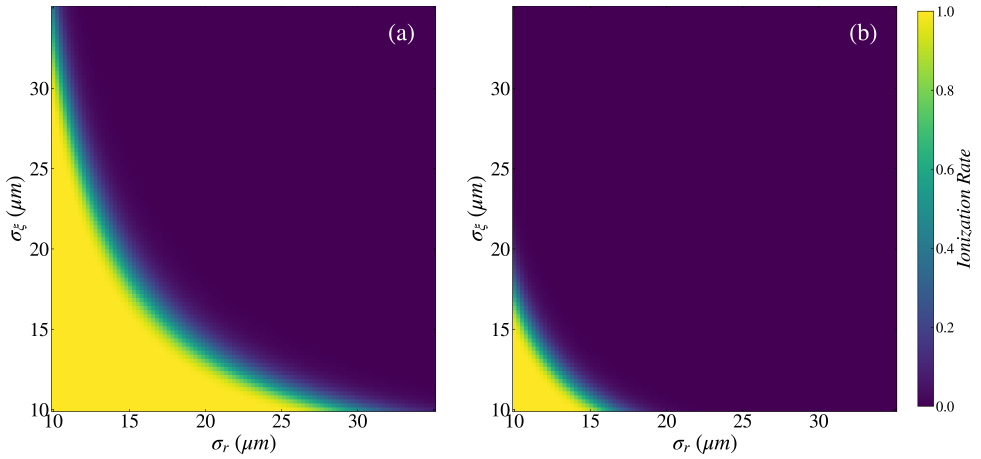

Figure 3. Ionization fraction due the electric field of an electron beam in (a) Hydrogen and (b) Helium calculated using the ADK approximation. The results show that a Gaussian beam with the current FACET-II beam parameters ($Q = 1.5\,\mathrm{nC}$, $\sigma_{x,y,z} = 20\,\mu\mathrm{m} \times 20\,\mu\mathrm{m} \times 20\,\mu\mathrm{m}$), does not ionize Hydrogen nor Helium.

and the narrow plasma column in Hydrogen. This tandem lens pair was initially designed for creating a wide plasma in Lithium vapor to achieve beam matching into the bulk plasma. The first lens (Tandem lens A in Fig.2) produces a donut-shaped intensity profile at the second lens. The second lens (Tandem lens B in Fig.2) removes the residual phase from the first lens [26, 27], and adds the required phase to create a Bessel-like, 70 cm long, 60 μm wide focus, designed to produce a uniform plasma column. The distance between the two lenses is 1 m. The lens pair is designed for a 40 mm diameter laser beam; yet, a smaller laser beam size can be used to shorten the length of the high-intensity focal region. Detailed discussion on the design and manufacture of the tandem lens can be found in reference [22].

We used a in-house code to model the 3D plasma profile generated by the laser [28, 22]. The ionization rate is determined using the ADK model, and the split-step Fourier (SSF) algorithm [29] takes into account the ionization refraction. Various gas density and laser intensity combinations are simulated to find a working point where both the wide and narrow plasma columns can be generated by the tandem lens pair. Table 2 shows the optical and gas parameters and Fig. 4 shows the laser intensity and plasma density profiles for each plasma source.

Table 2. Laser and Gas parameters for the Simulated Wide and Narrow Plasma Sources

Variables	Narrow Plasma	Wide Plasma
Plasma Source Transverse FWHM	53.2 μm	295.5 μm
Plasma Source Length	$\approx$ 750 mm	$\approx$ 750 mm
Species	Hydrogen	Hydrogen
Gas Density (Full ionization plasma den.)	5 $\times 10^{16}\mathrm{cm}^{-3}$	5 $\times 10^{16}\mathrm{cm}^{-3}$
Optics Used	Tandem lens pair	Tandem lens pair
Laser Power (On Target)	28 mJ	262.5 mJ
Pulse Duration (FWHM)	55 fs	55 fs
Laser Spot Size	20.24 mm	14.00 mm

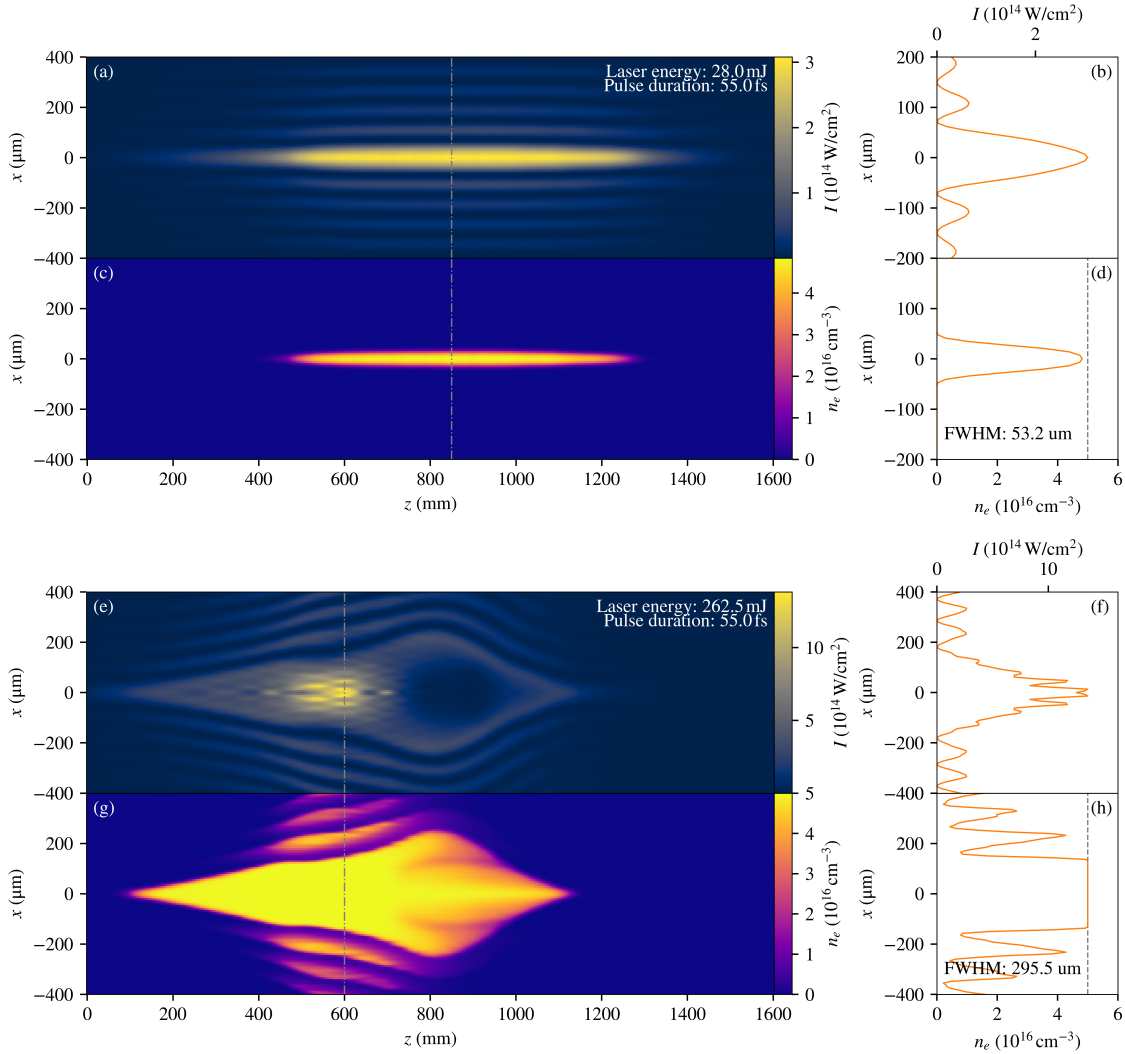

Figure 4. Laser ionization of the Hydrogen plasma sources utilizing the custom-designed tandem lens pair is simulated using a in-house split-step Fourier code. The reference point, $z = 0$, is positioned 1.25 m downstream of the second diffractive optic (tandem lens B in Fig. 2). Different laser intensities are applied to generate narrow and wide plasma columns. The plasma length is adjusted and matched by varying the incoming laser spot size. (a) illustrates the intensity profile of the central temporal slice of the laser pulse on the $y = 0$ plane for the narrow plasma, while (b) shows a lineout of the laser intensity at the middle of the plasma region. (c) presents the plasma density profile on the $y = 0$ plane for the narrow plasma, and (d) shows a lineout of the transverse plasma profile, which has a FWHM of 53.2 μm. Similarly, panels (e-h) depict the simulated results for the wide-column plasma.

3.3. Experimental Signature

To study the wakefield structure of the narrow column PWFA using the initially available single-bunch electron beam at FACET-II, we would ideally stretch the bunch length to probe the full longitudinal extent of the first wake period and the trailing sheath electrons. There are two primary constraints to this scheme. First, the PWFA must remain in the blowout regime ($n_b \geq 2n_0$). Second, the bunch length must be as long as the blowout wake period ($2\sigma_\zeta \geq \lambda_p$).

Figure 5 shows that a longitudinally stretched, 1.5 nC, Gaussian beam with radius $\sigma_r = 20$ μm cannot simultaneously meet both criteria.

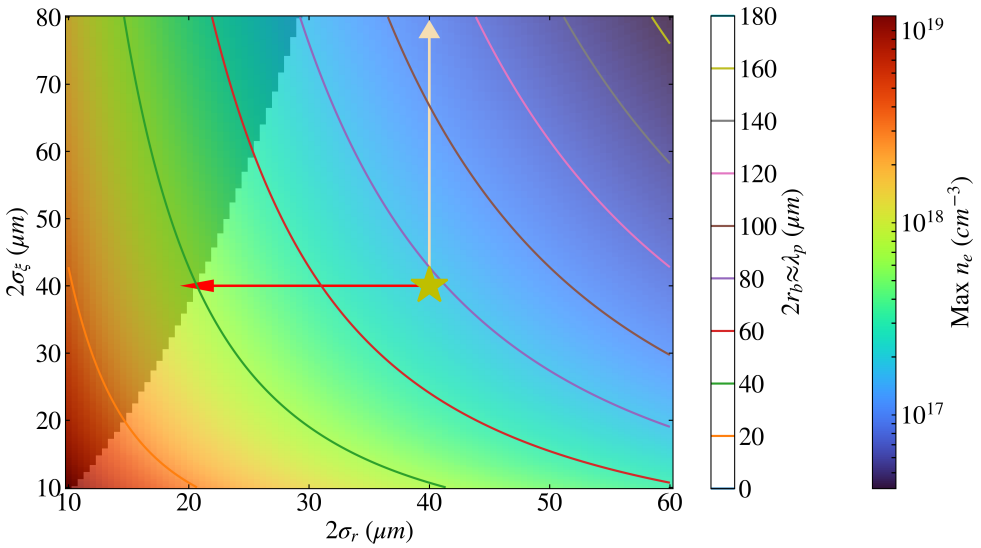

Figure 5. The color scale shows the maximum plasma density in which a Gaussian drive beam of transverse size σ_r and longitudinal size σ_ζ can drive a nonlinear wake ($n_b \geq 2n_0$). The contour lines indicate the blowout diameter corresponding to the given plasma density. The darker shaded regime is where the beam tail can sample the entire extent of the blowout wake: $2\sigma_\zeta \geq 2r_b$, where r_b is the blowout radius. The star symbol represents the current FACET-II beam parameters ($\sigma_{r,z} = 20, 20$ μm), situated well outside the gray region. Stretching the beam to a longitudinal size of $\sigma_z = 40$ μm, as indicated by the yellow arrow, will not position it within the gray area. Conversely, when FACET-II can produce beams with reduced transverse dimensions (highlighted by the red arrow), it becomes feasible to investigate the trailing sheath electrons using a single bunch in a higher plasma density.

Although our calculation indicates that the stretched beam is not able to cover the entire wake period while maintaining a blowout wake, we still expect a distinct difference in the strength of the deaccelerating field between the narrow and wide plasma columns. To study the experimental signatures, we simulated the FACET-II beam (beam parameters shown in table 1) traversing through a 70 cm-long plasma with two different radii (narrow, $2r_p = 55$ μm; wide, $2r_p = 160$ μm) via PIC simulations. The resultant beam density, plasma density, longitudinal and transverse electric fields are shown in Fig 1. The final energy of the electron beams are shown in Fig. 6. A clear difference in energy loss should provide a strong experimental signature for the successful demonstration of a narrow column PWFA.

Even though 18% of the charge in the drive beam is initially outside the narrow plasma column, the transverse focusing field from the wake could quickly focus the beam down to a smaller spot size. This process would result in a comparable amount of charge contributes to the wake's generation in wide- and narrow- plasma columns. In this case, the observed variation in the longitudinal wakefield mainly arises from reduced plasma sheath electron current in narrower plasma columns compared to the wide ones. Furthermore, the plasma columns utilized in the presented PIC simulations are characterized by a step function density profile. A more realistic radial plasma ramp profile will be implemented in future work.

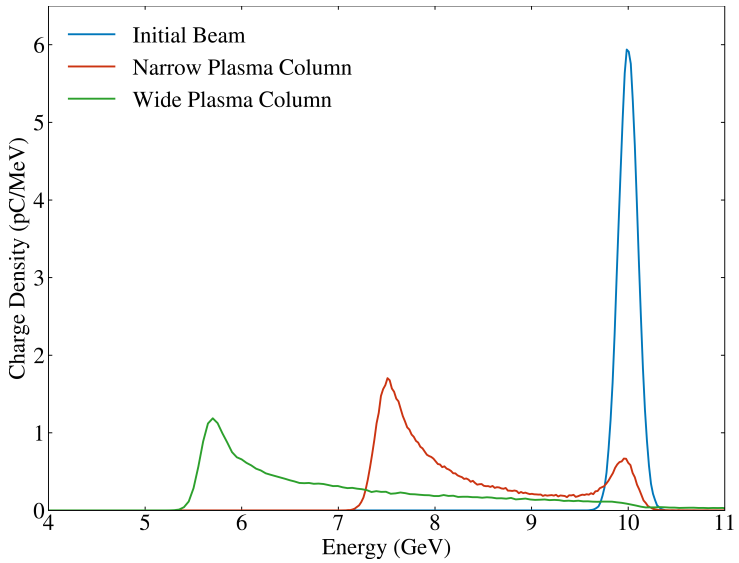

Figure 6. Electron beam energy of (a) the initial single-bunch beam, (b) the beam after traversing a 70 cm, $5 \times 10^{16}\,\mathrm{cm}^3$, narrow ($2r_p = 55\,\mu$m) plasma column, and (c) the beam after traversing a wide ($2r_p = 160\ \mu$m) plasma column of the same density and length, simulated via a PIC simulation presented in Fig. 1. The difference in energy loss provides a clear experimental signature of the narrow column PWFA.

4. Misalignment Study

In this Section, we study the effect of misalignment between the incoming electron beam and the plasma column. The two primary sources of misalignment are the pointing jitter of the ionizing laser pulse and the transverse position of the incoming electron beam. The former causes the plasma column and the electron beam trajectory to be misaligned by a polar angle θ and a coupled offset $d \cdot \theta$, where $d = 1.4$ m is the distance between the final focusing optic to the beginning of the plasma. The offsets and tilts induced by laser jitter are coupled, and always have the same sign. The electron position jitter causes an offset between the plasma column and the electron beam trajectory.

Recent measurements at FACET-II suggest that the laser has a pointing jitter of $\pm \sim 10\ \mu$rad RMS in both transverse dimensions and the electron beam position jitter is aimed to be $\pm 5\ \mu$m RMS. This indicates that the centroid of the electron beams will arrive within the radius of the narrow plasma column approximately 82% of the time, and within the wide column 100% of the time. Previous research [30] suggests that an electron beam travelling parallel to–but outside of–a plasma filament will be attracted toward the filament when a wake is driven in the plasma. We also observed this behavior in our simulations. We therefore expect to observe an interaction between the electron beam and the plasma in nearly all shots.

Figure 7 (a-c) and (d-f) show the evolution of the beam-plasma interaction when the laser has a 10 μrad angular misalignment with a coupled offset of 14 μm in a wide and narrow plasma column, respectively. In both cases, the electron beam remains within the plasma throughout its propagation due to the attractive force of the ion column. Because the sign of the offset and the angular tilt are the same, the electron beam will always enter the plasma at its start or miss the plasma entirely, never entering the plasma part way down its length, assuming the beams are perfectly aligned to begin with and do not drift over time. This gives confidence that the difference in the final spectrum of the electron beam in the wide and narrow plasma sources arises only from the difference in their respective wakefields rather than the length of

their interaction.

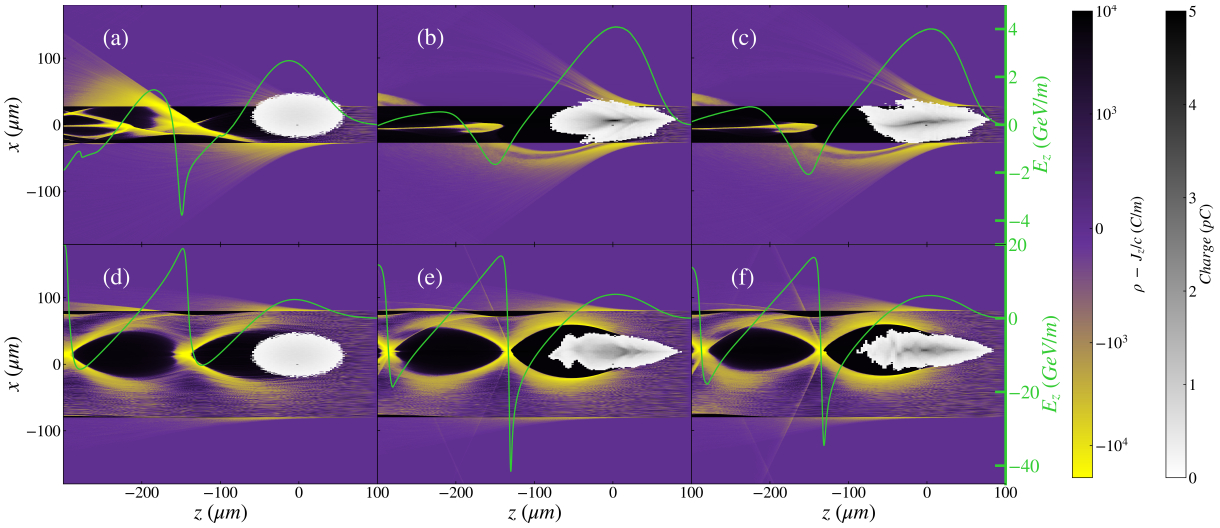

Figure 7. The top row shows the plasma electron density (purple/yellow colormap), the drive electron bunch density (black/white colormap), and the longitudinal field lineout at the centroid of the drive bunch (green curve) of a narrow plasma column ($2r_p = 55\,\mu$m) PWFA where the e-beam and the plasma column are misaligned (the e-beam is offset by $14.3\,\mu$m and tilted up by $10\,\mu$rad, corresponding to a $10\,\mu$rad laser-e-beam misalignment) at various propagation distances, (a) $z = 0$ cm, (b) $z = 35$ cm, and (c) $z = 70$ cm. Similarly, (d), (e), and (f) show the wide plasma column ($2r_p = 160\,\mu$m) PWFA case with the same misalignment. The e-beam is guided by the narrow-column plasma, and the offset with respect to the center of the plasma column decreases from $14.3\,\mu$m to $4.5\,\mu$m in the narrow plasma column. Meanwhile, the offset increases from $14.3\,\mu$m to $21.3\,\mu$m as expected with a 10μrad upward tilt in the wide plasma column, showing no signs of guiding.

Figure 8 (a-c) and (d-f) show the final spectrum and transverse position of the electron beam after propagation through the narrow and wide plasma PWFA, respectively. Each colored line represents a different initial polar angle θ misalignment of the ionization laser. Subfigures (a) and (d) show that the final energy spectrum in each case is relatively insensitive to the misalignment and therefore able to provide a clear indication of the variation of the plasma width, as was predicted in the previous Section. Subfigures (b) and (e) show that the narrow plasma column has a guiding effect on the electron beam, while the wide plasma column has little effect on the propagation direction of the beam. Subfigures (b) and (e) illustrate the anticipated correlation between laser jitter, measurable with a far-field laser camera, and the transverse position at which electrons exit, determinable via electron energy spectra in a narrow plasma column. Conversely, this correlation is absent in a wide plasma. This guiding effect provides another experimental signature that can provide strong evidence of propagation through a narrow plasma column.

5. Conclusions and Future Work

The ultimate goal of the E333 experiment at FACET-II is to accelerate positrons in a narrow column PWFA. Initial experiments will test the narrow column PWFA using the currently available single-bunch electron beam. Calculations and simulations show that the narrow plasma column can be formed by laser ionization and that proper selection of the bunch parameters will prevent additional beam ionization that would widen the plasma column. The primary observable signatures for this stage of the experiment are the final energy spectrum and

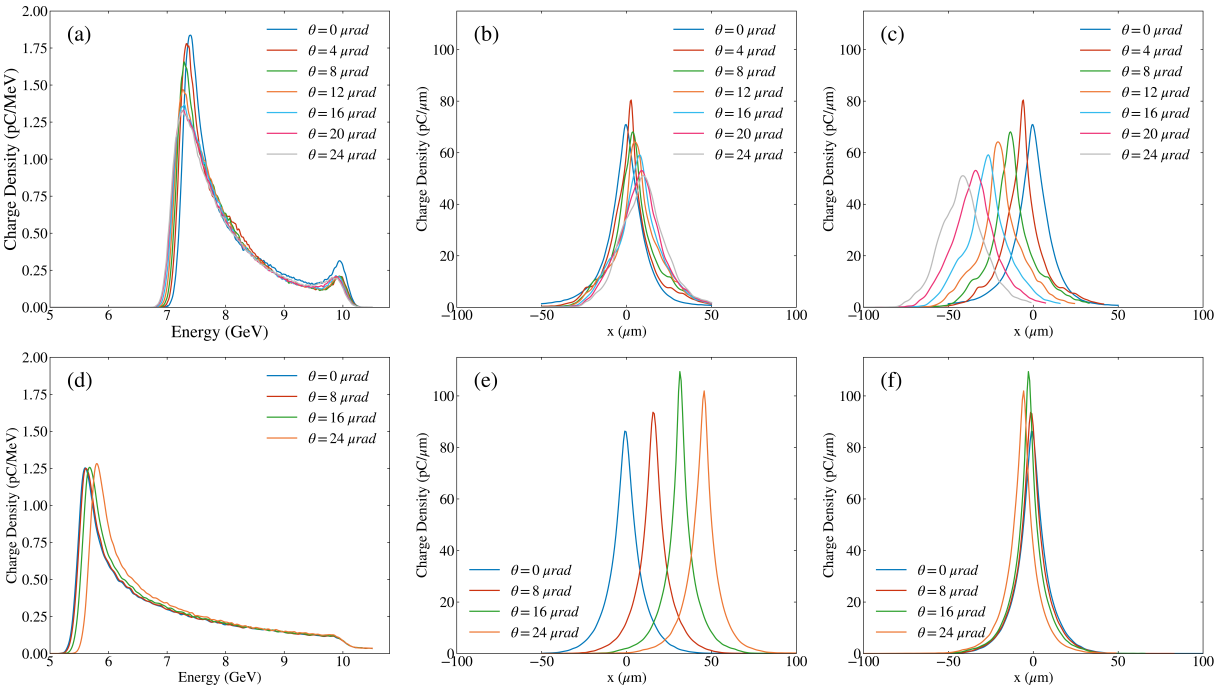

Figure 8. We simulate the e-beam interacting with a 70-cm long, laser-ionized, narrow ($2r_p = 55\,\mu$m) plasma column (a, b, c), and wide ($2r_p = 160\,\mu$m) plasma column (d, e, f). The curves in each figure correspond to various laser-e-beam misalignments, with θ being the polar angle between the laser-axis and the e-beam-axis. Each angular misalignment couples with a centroid offset of $d \cdot \theta$, where $d = 1.4$ m. The laser-e-beam misalignment is on the y=0 plane to maximize the observability of the misalignment effects in the x direction. (a) shows the energy spectrum. (b) shows the projected transverse position of the electron beam at the exit of the plasma column in the laser frame, and (c) shows the projected transverse position of the electron beam in the lab frame. (d), (e), and (f) show the same experimental signature in the wide plasma column case. (a) and (d) indicates that the difference of the drive bunch energy lost in a narrow plasma versus a wide plasma is observable even when the laser is misaligned by 24 μrad, which should correspond to $\sim 95\%$ of shots observed at FACET-II. (b) demonstrates that the narrow plasma column guides the e-beam, so the e-beam exits the plasma near the center of the column ($x \sim 0$ in the laser frame), while (e) shows no guiding effect. Finally, (b) is converted to the lab frame and plotted in (c), where the projected e-beam exit position is strongly correlated with the laser pointing jitter.

transverse position of the electron bunch as measured at the electron spectrometer. The total amount of energy loss is expected to be significantly lower in the case of the narrow plasma column. In addition, the narrow column PWFA is expected to provide transverse guiding of the electron beam, yielding a strong correlationhigh between the exiting beam trajectory and the laser pointing jitter.

Following the single electron bunch experiment, we plan to investigate the narrow column PWFA with a two-bunch electron beam structure. The drive beam will drive a wake in the narrow plasma, creating an elongated electron filament in the rear of the wake. The witness beam will be loaded at various longitudinal positions to study the wakefield structure. When loaded within the first wake bubble, the witness beam will be focused and accelerated. When it is loaded beyond the rear of the first wake period within the extended plasma electron filament, the witness beam is expected to be rapidly defocused. This may make it challenging to detect on the

spectrometer screen due to low charge density and the potential of charge loss in apertures during transport. Loading the witness beam behind the filament should result in transverse focusing and deceleration. This two-bunch experiment will be the first experimental measurement of the elongated electron filament in a narrow-column PWFA. Direct measurement of the extended electron filament will confirm the simulation results and verify that the plasma is performing as expected before attempting to accelerate positrons.

Acknowledgement

This material is based upon work supported by the U.S. Department of Energy, Office of Science, Office of High Energy Physics, under Award Number DE-SC001796, and by the National Science Foundation under Grant Number PHY-2047083. This research used resources of the National Energy Research Scientific Computing Center, a DOE Office of Science User Facility supported by the Office of Science of the U.S. Department of Energy under Contract No. DE-AC02-05CH11231 using NERSC award HEP-ERCAP0024521. Work at LBNL is supported by the Director, Office of Science, Office of High Energy Physics, of the U.S. Department of Energy, under Contract No. DE-AC02–05CH11231

References

[1] Litos M *et al.* 2016 *Plasma Physics and Controlled Fusion* **58**(3) 034017
[2] Blumenfeld I *et al.* 2007 *Nature* **445**(7129) 741–744
[3] Litos M *et al.* 2014 *Nature* **515**(7525) 92–95
[4] Lindstrøm C A *et al.* 2021 *Phys. Rev. Lett.* **126**(1) 014801
[5] Schroeder C B, Esarey E, Geddes C G R, Benedetti C and Leemans W P 2010 *Phys. Rev. ST Accel. Beams* **13**(10) 101301
[6] Rosenzweig J B, Breizman B, Katsouleas T and Su J J 1991 *Phys. Rev. A* **44**(10) R6189–R6192
[7] Blue B E *et al.* 2003 *Phys. Rev. Lett.* **90**(21) 214801
[8] Corde S *et al.* 2015 *Nature* **524** 442–445
[9] Gessner S *et al.* 2016 *Nature communications* **7** 11785
[10] Gessner S *et al.* 2023 *arXiv preprint arXiv:2304.01700*
[11] Lindstrøm C A *et al.* 2018 *Phys. Rev. Lett.* **120**(12) 124802
[12] Lotov K 2007 *Physics of plasmas* **14** 023101
[13] Zhou S, An W, Ding S, Hua J, Mori W B, Joshi C and Lu W 2022 *arXiv preprint arXiv:2211.07962*
[14] Diederichs S, Benedetti C, Huebl A, Lehe R, Myers A, Sinn A, Vay J L, Zhang W and Thévenet M 2022 *Computer Physics Communications* **278** 108421
[15] Lee V 2024 *10.5281/zenodo.10816197*
[16] Diederichs S, Mehrling T J, Benedetti C, Schroeder C B, Knetsch A, Esarey E and Osterhoff J 2019 *Phys. Rev. Accel. Beams* **22**(8) 081301
[17] Diederichs S, Benedetti C, Esarey E, Osterhoff J and Schroeder C B 2020 *Phys. Rev. Accel. Beams* **23**(12) 121301
[18] Diederichs S, Benedetti C, Thévenet M, Esarey E, Osterhoff J and Schroeder C B 2022 *Phys. Rev. Accel. Beams* **25**(9) 091304
[19] Diederichs S, Benedetti C, Esarey E, Thévenet M, Osterhoff J and Schroeder C B 2022 *Physics of Plasmas* **29** 043101
[20] Yakimenko V *et al.* 2019 *Phys. Rev. Accel. Beams* **22**(10) 101301
[21] Storey D *et al.* 2023 *arXiv preprint arXiv:2310.06215*
[22] Ariniello R 2022 *Emittance Preservation in a Plasma Wakefield Accelerator* Ph.D. thesis University of Colorado, Boulder
[23] Gessner S 2020 *SLAC National Accelerator Laboratory FACET-II PROPOSAL Positron Acceleration in an Electron Beam-Driven Plasma Filament Wakefield*
[24] Keldysh L 1965 *Sov. Phys. JETP* **20** 1307–1314
[25] Zhang C, Storey D, Claveria P S M, Nie Z, Marsh K, Hogan M, Mori W, Adli E, An W, Ariniello R *et al.* 2024 *Plasma Physics and Controlled Fusion* **66** 025013
[26] Honkanen M and Turunen J 1998 *Optics Communications* **154** 368–375
[27] Ouadghiri-Idrissi I, Giust R, Froehly L, Jacquot M, Furfaro L, Dudley J M and Courvoisier F 2016 *Optics Express* **24**(11) 11495–11504 ISSN 10944087

[28] Lee V, Ariniello R, Doss C, Wolfinger K, Stoltz P, Hansel C, Gessner S, Cary J and Litos M 2024 *Physics of Plasmas* **31** 013104
[29] Stoffa P, Fokkema J T, de Luna Freire R and Kessinger W 1990 *Geophysics* **55** 410–421
[30] Adli E *et al.* 2016 *New Journal of Physics* **18** 103013

ChatGPT 3.5 and 4.0 has been used for spell check, minor language editing, and python functions generation. The first author takes full responsibility for the content of my manuscript.